First Examples of a Dithiolato Bridge in (η^6-C_6Me_6)Ru^{II}−$Cr^{0,II,III}$ Complexes. Synthetic, Single-Crystal X-ray Diffraction, and Electrochemical Studies

Richard Yee Cheong Shin, Victor Wee Lin Ng, Lip Lin Koh, Geok Kheng Tan, Lai Yoong Goh,*,# and Richard D. Webster

Department of Chemistry, National University of Singapore, Kent Ridge, Singapore 117543, and Division of Chemistry and Biological Chemistry, Nanyang Technological University, Singapore 637616

Received May 14, 2007

The interactions of [(HMB)Ru^{II}{η^3-tpdt)}] (**1**) [HMB = η^6-C_6Me_6, tpdt = $S(CH_2CH_2S^-)_2$] with $Cr(CO)_6$, $[CpCr(CO)_3]_2$, $[CpCrCl_2(SPyH)]$, and $[Cp^*Cr(CH_3CN)_4](PF_6)_2$ (**6**) produced a series of thiolate-bridged Ru−Cr heterobimetallic complexes: viz., [{(HMB)Ru(μ-η^2:η^3-tpdt)}{$Cr(CO)_4$}] (**3**), [{(HMB)-Ru(μ-η^2:η^3-tpdt)}{$CpCr(CO)_2$}][$CpCr(CO)_3$] (**4**), [{(HMB)Ru(μ-η^2:η^3-tpdt)}{CpCrCl}](PF_6) (**5**), and [{(HMB)Ru(μ-η^2:η^3-tpdt)}{Cp*Cr(MeCN)}]$(PF_6)_2$ (**8**), in respective yields of 29%, 67%, 62%, and 79%. Complex **6** was synthesized from $[Cp^*CrBr_2]_2$ and found to readily convert to $[Cp^*Cr\{(CH_3)_2CO\}_3]$-$[Cp^*Cr\{(CH_3)CO\}_2(MeCN)](PF_6)_4$ (**7**) upon recrystallization from acetone. Each compound could be electrochemically oxidized and reduced in several one-electron or multiple-electron steps. The voltammetric responses were complicated and varied depending on the electrode surface and temperature. The single-crystal X-ray structures of **3**−**5**, **7**, and **8** have been determined.

1. Introduction

The keen interest in transition-metal complexes containing sulfur ligands is linked to their relevance in biological and industrial processes.[1] Of special significance in applications as catalyst precursors in both homogeneous and heterogeneous catalysis are heterobimetallic compounds,[2] which often contain bridging monothiolate (RS^-)[3] but rarely bridging dithiolate ($^-SRS^-$)[4] ligands. Thiolate bridging of the dithiolate−thioether ligand 3-thiapentane-1,5-dithiolate, $S(CH_2CH_2S^-)_2$ (tpdt), had been found in dinuclear coordination compounds of Ni(II)[5] and In(III)[6] with μ-SR linkages and of Ni/Fe wherein Ni(NO)(tpdt) functions as a dithiolato chelate to Fe.[7] Shortly after we encountered such a bonding mode of M(tpdt) in an organometallic complex obtained from the reaction of the areneruthenium complex [(HMB)Ru^{II}(η^3-tpdt)] (**1**) [HMB = η^6-C_6Me_6] with the μ-dichlorido complex $[(HMB)RuCl_2]_2$ (**A**) (Scheme 1).[8] We have since obtained numerous examples illustrating the strong tendency of **1** to function as a metalloligand toward metal fragments, via facile cleavage and displacement of chlorido ligands in Ru(II) complexes, such as **A** or $[Ru^{II}(COD)Cl_2]_n$ (**B**) (Scheme 1). In reactions with the μ-dichloridoruthenium(III) complex $[Cp^*RuCl_2]_2$ (**C**), the additional participation of Ru(II)−Ru(III) redox reactions led to homodi- and homotrinuclear complexes, shown in Scheme 2.[9]

Scheme 1

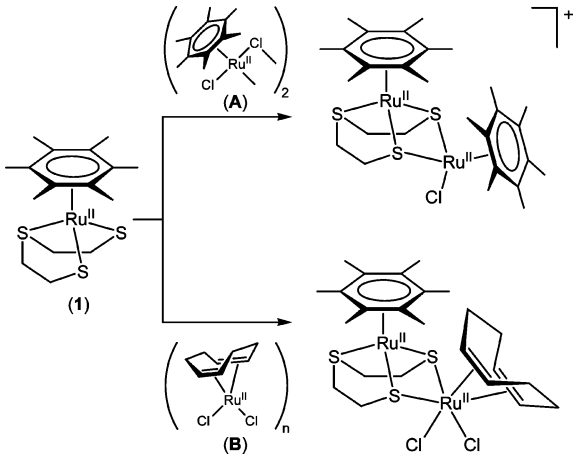

* To whom correspondence should be addressed at the National University of Singapore. E-mail: laiyoonggoh@ntu.edu.sg. Fax: (+65) 67791691. Phone: (+65) 65162677.

Current address: Division of Chemistry and Biological Chemistry, Nanyang Technological University, Singapore 637616.

(1) See, for instance, the following and references therein: (a) *Transition Metal Sulfur Chemistry—Biological and Industrial Significance*; Stiefel, E. I., Matsumoto, K., Eds.; ACS Symposium Series 653; American Chemical Society: Washington, DC, 1996. (b) Sellman, D.; Sutter, J. *Acc. Chem. Res.* **1997**, *30*, 460. (c) Dubois, M. R. *Chem. Rev.* **1989**, *89*, 1. (d) Bianchini, C.; Meli, A. *Acc. Chem. Res.* **1998**, *31*, 109. (e) Ogino, H.; Inomata, S.; Tobita, H. *Chem. Rev.***1998**, *98*, 2093.

(2) See for instance the following and references therein: (a) Braunstein, P.; Rosé, J. In *Comprehensive Organometallic Chemistry II*; Wilkinson, G., Stone, F. G. A., Abel, E. W., Eds.; Pergamon: Oxford, 1995; Vol. 10, p 351. (b) *The Chemistry of Heteronuclear Clusters and Multimetallic Catalysts*; Adams, R. D., Herrmann, W. A., Eds. *Polyhedron* **1988**, *7*, 2251. (c) Wheatley, N.; Kalck, P. *Chem. Rev.* **1999**, *99*, 3379. (d) Guczi, L. In *Metal Clusters in Catalysis*; Gates, B. C., Guczi, L., Knozinger, H., Eds.; Elsevier: New York, 1986. (e) Holt, M. S.; Wilson, W. L.; Nelson, J. H. *Chem. Rev.* **1989**, *89*, 11.

(3) See for instance the following and references therein: (a) Stephan, D. W. *Coord. Chem. Rev.* **1989**, *95*, 41. (b) Janssen, M. D.; Grove, D. M.; Van Koten, G. *Prog. Inorg. Chem.* **1997**, *46*, 97. (c) Darensbourg, M. Y.; Pala, M.; Houliston, S. A.; Kidwell, K. P.; Spencer, D.; Chojnacki, S. S.; Reibenspies, J. H. *Inorg. Chem.* **1992**, *31*, 1487. (d) Yam, V. W.-W.; Wong, K. M.-C.; Cheung K.-K. *Organometallics* **1997**, *16*, 1729. (e) Rousseau, R.; Stephan, D. W. *Organometallics* **1991**, *10*, 3399.

(4) (a) Aggarwal, R. C.; Mitra, R. *Indian J. Chem.* **1994**, *A33*, 55. (b) Nadasdi, T. T.; Stephan, D. W. *Inorg. Chem.* **1994**, *33*, 1532.(c) Forniés-Cámer, J.; Masdeu-Bultó, A. M.; Claver, C.; Tejel, C.; Ciriano, M. A.; Cardin, C. J. *Organometallics* **2002**, *21*, 2609 and references therein.

(5) (a) Harley-Mason, J. *J. Chem. Soc.* **1952,** 146. (b) Barclay, G. A.; McPartlin, E. M.; Stephenson, N. C. *Aust. J. Chem.* **1968**, *21*, 2669 and references therein.

(6) Kim, J.-H.; Huang, J.-W.; Park, Y.-W.; Do, Y. *Inorg. Chem.* **1999**, *38*, 353.

(7) Liaw, W.-F.; Chiang, C.-Y.; Lee, G.-H.; Peng, S.-M.; Lai, C.-H.; Darensbourg, M. Y. *Inorg. Chem.* **2000**, *39*, 480.

(8) Shin, R. Y. C.; Bennett, M. A.; Goh, L. Y.; Chen, W.; Hockless, D. C. R.; Leong, W. K.; Mashima, K.; Willis, A. C. *Inorg. Chem.* **2003**, *42*, 96.

10.1021/om700474k CCC: $37.00
Publication on Web 07/31/2007

Scheme 2

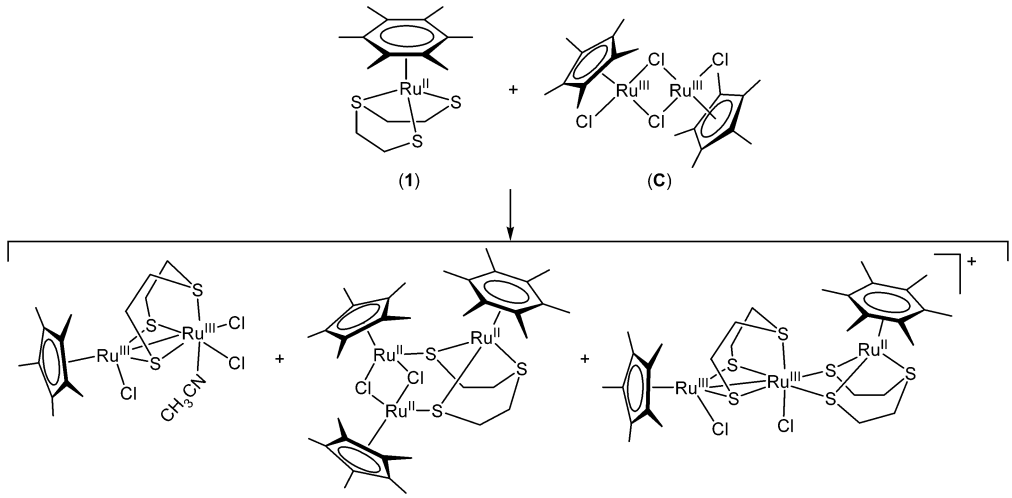

Scheme 3

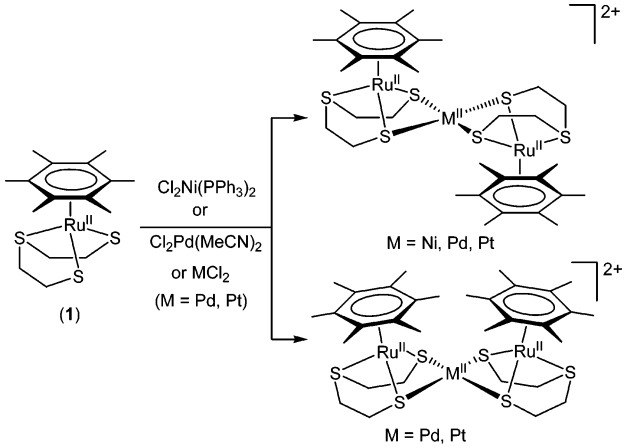

Scheme 4

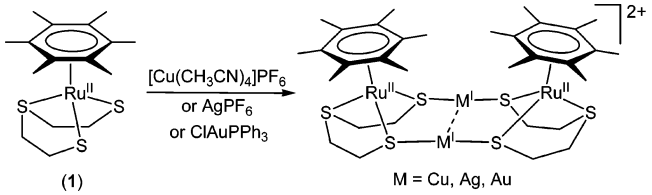

Scheme 5

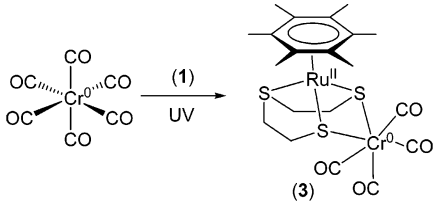

Displacement of chlorido and/or phosphane (or solvento) ligands from group 10 coordination compounds gave heterometallic derivatives, in which the dithiolate tpdt moiety chelates to the group 10 metal,[10] with both *trans* and/or *cis* configuration in the trinuclear "adducts" (Scheme 3). With group 11 metal fragments,[11] tetranuclear annular complexes, stabilized by metallophilic interactions, are formed (Scheme 4). Likewise, [(η^5-C_5Me_5)Ru^{III}(η^3-tpdt)] (**2**), the Ru(III) analogue of **1,** functions efficiently as a metallodithiolato chelating ligand.[12]

We note that Cr−Ru complexes (bridged or unbridged) are rare, compared to Mo−Ru compounds.[13] This is surprising, considering that mixed-metal compounds of groups 6 and 8 are of special interest from a catalytic perspective, owing to the different properties of the two groups of metals, e.g., oxophilicity of the former and the hydrogen activation ability of the latter.[1c,14] In particular, thiolato complexes of Cr with Ru are barely known. To the best of our knowledge, the only case of a thiolato-bridged Cr−group 8 metal is $CpFe(CO)_2(\mu$-SPh)$Cr(CO)_5$.[15]

Our previous encounters with the efficacious bidentate ligation of complex **1** to various metal centers prompted us to examine this particular reactivity feature of **1** toward Cr in various oxidation states, with an intention to also investigate the electrochemistry of the ensuing products. In this paper we describe the results.

2. Results and Discussion

We selected chromium substrates in various oxidation states to react with **1**, viz., $Cr^0(CO)_6$, $[CpCr^I(CO)_3]_2$, $CpCr^{III}Cl_2$(SPyH), and $[Cp^*Cr^{III}Br_2]_2$.

The reaction of **1** with $Cr(CO)_6$ proceeded under UV photolytic conditions. As the reaction progressed, orange solids of [{(HMB)Ru(μ-η^2:η^3-tpdt)}{$Cr(CO)_4$}] (**3**) precipitated out of solution, with 29% yield after 3 h (Scheme 5). X-ray diffraction analysis of **3** shows chelation of the dithiolato sulfur atoms of tpdt of **1** to a $Cr(CO)_4$ unit, as shown in the ORTEP diagram in Figure 1. The coordination environment at Cr resembles those in $[Cr^0(CO)_4(S_2C_6R_4)]^{2-}$ (R = H, Cl, Me)[16]

(9) Shin, R. Y. C.; Ng, S. Y.; Tan, G. K.; Koh, L. L.; Khoo, S. B.; Goh, L. Y.; Webster, R. D. *Organometallics* **2004**, *23*, 547.

(10) (a) Shin, R. Y. C.; Tan, G. K.; Koh, L. L.; Goh, L. Y.; Webster, R. D. *Organometallics* **2004**, *23*, 6108. (b) Shin, R. Y. C.; Teo, M. E.; Tan, G. K.; Koh, L. L.; Vittal, J. J.; Goh, L. Y.; Murray, K. S.; Moubaraki, B.; Zhou, Z. Y. *Organometallics* **2005**, *24*, 4265.

(11) Shin, R. Y. C.; Tan, G. K.; Koh, L. L.; Vittal, J. J.; Goh, L. Y.; Webster, R. D. *Organometallics* **2005**, *24*, 539.

(12) Shin, R. Y. C.; Goh, L. Y. *Acc. Chem. Res.* **2006**, *39*, 301.

(13) (a) Wilkinson, G., Stone, F. G. A., Abel, E. W., Eds. *Comprehensive Organometallic Chemistry II*; Pergamon: Oxford, 1995; Vol. 10, Chapter 2 (Chetcuti, M. J.) and Chapter 3 (Chi, Y.; Hwang, D.-K.). (b) Straub, T.; Haukka, M.; Pakkanen, T. A. *J. Organomet. Chem*. **2000**, *612*, 106 and references therein.

(14) (a) Chaudret, B.; Dahan, F.; Sabo, S. *Organometallics* **1985**, *4*, 1490. (b) Shapley, P. A.; Zhang, N. Z.; Allen, J. L.; Pool, D. H.; Liang, H.-C. *J. Am. Chem. Soc.* **2000**, *122*, 1079.

(15) Hossain, M. M.; Lin, H.-M.; Shyu, S.-G. *Eur. J. Inorg. Chem*. **2001**, 2655.

(16) Sellmann, D.; Wille, M.; Knoch, F. *Inorg. Chem*. **1993**, *32*, 2534.

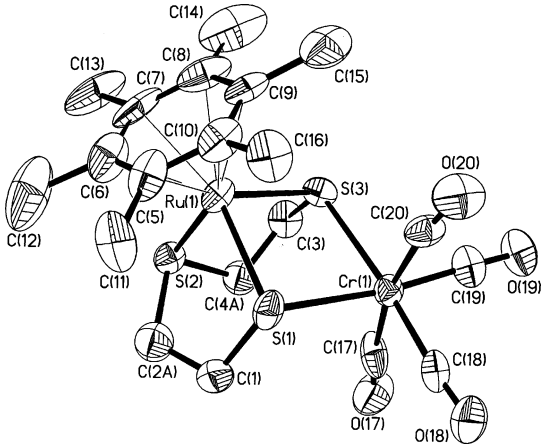

Figure 1. ORTEP diagram for **3** (50% probability thermal ellipsoids, hydrogen atoms omitted for clarity).

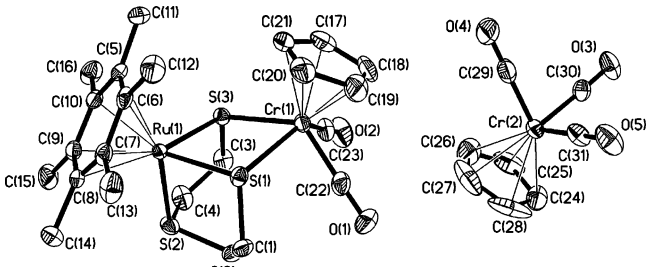

Figure 2. ORTEP diagram for **4** (50% probability thermal ellipsoids, hydrogen atoms omitted for clarity).

Scheme 6

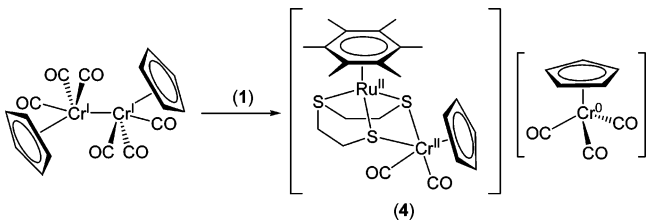

and $[Cr^0(CO)_4(S_2CC(PPh_3)_2)]$,[17] both of which contain a chelating dithiolato ligand. These two complexes exhibit four (range 1980−1760 cm^{-1}) and three (range 1988−1810 cm^{-1}) ν(CO) absorptions, respectively. These frequencies agree very well with those we observed for **3** (1986, 1851, and 1817 cm^{-1}). We note that these CO stretching frequencies are significantly lower than those in *cis*-$L_2Cr(CO)_4$ containing N-donor ligands, e.g., for L = isonitriles, RNC (ν(CO) in range 2022−1921 cm^{-1}),[18] and L_2 = bidentate isocyano, di-NC (ν(CO) in range 2009−1932 cm^{-1}).[19] This difference is in accord with the better σ-donor capability of S versus N.

The stoichiometric reaction of **1** and $[CpCr(CO)_3]_2$ at ambient temperature resulted in the isolation of a salt complex, [{(HMB)-Ru(μ-η^2:η^3-tpdt)}{$CpCr(CO)_2$}][$CpCr(CO)_3$] (**4**), in moderate yield (Scheme 6). Single-crystal diffraction analysis confirms the presence of a cationic Ru−Cr moiety with both Ru and Cr in the +2 oxidation state and a counteranion, $[CpCr(CO)_3]^-$, containing Cr(0) (Figure 2). This clearly indicates that Cr(I) in $[CpCr(CO)_3]_2$ has disproportionated into Cr(0) and Cr(II). We

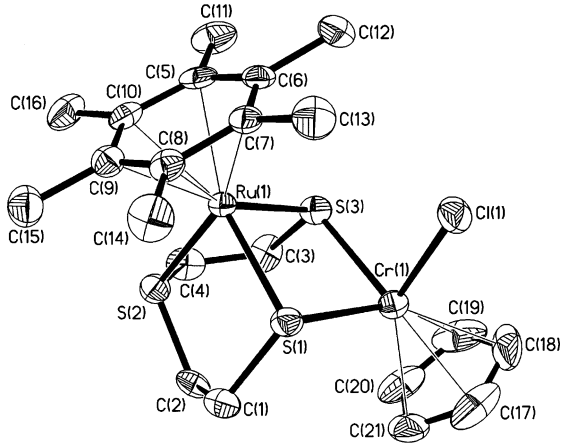

Figure 3. ORTEP diagram for the cation of **5** (50% probability thermal ellipsoids, hydrogen atoms omitted for clarity).

Scheme 7

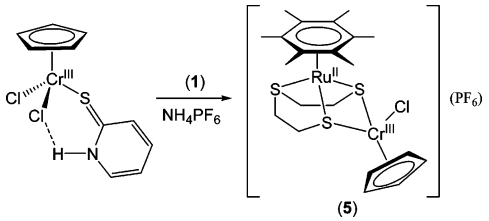

note that disproportionation has been demonstrated to be a recurring phenomenon accompanying substitution reactions of this Cr dimer.[20] The coordination environment at Cr in **4** resembles somewhat that in the diphosphane analogues [CpCr-$(CO)_2$(P−P)][$CpCr(CO)_3$] (P−P = $Ph_2(CH_2)_nPh_2$ for n = 1, 2, and 4); these exhibit three to five CO stretches between 1976 and 1751 cm^{-1} in CH_2Cl_2, with the two lower frequency stretches being assigned to the anion.[20] Likewise, **4** in a KBr pellet shows four CO stretches between 1944 and 1757 cm^{-1}, with those at 1867 and 1757 cm^{-1} likely belonging to the anion, though the Δ of 30 cm^{-1} toward lower frequency from those of Na[$CpCr(CO)_3$] cannot be easily rationalized. The remaining two stretches at 1944 and 1882 cm^{-1}, assignable to the cationic Ru−Cr moiety, are 20−30 cm^{-1} lower than those in the phosphane analogues, in agreement with the higher donor capability of the S atoms of the bridging tpdt ligand.

The stoichiometric reaction of **1** with the thione complex [$CpCrCl_2$(SPyH)] at ambient temperature, followed by metathesis using NH_4PF_6, resulted in the isolation of [{(HMB)Ru-(μ-η^2:η^3-tpdt)}{CpCrCl}](PF_6) (**5**) in moderately high yield (Scheme 7). This reaction has involved the displacement of a chlorido and the labile 2-thionepyridinium ligands from the Cr center. This is confirmed by the X-ray crystal structure analysis, which shows the CpCr moiety is coordinated to a chlorido ligand and the dithiolato S atoms of tpdt of complex **1** (see the ORTEP diagram in Figure 3).

Having $[Cp^*CrBr_2]_2$ available in our laboratory, we attempted its reaction with **1**, hoping to get the bromido analogue of complex **5**. However, no reaction occurred, not unexpected on account of the strong Cr(III)−Br bond. We next converted it into a solvento analogue of **5** with use of $AgPF_6$ as a bromide abstractor in acetonitrile. Indeed, an instantaneous reaction occurred, giving an extremely air-sensitive deep red solution from which was isolated complex **6** (Scheme 8). This compound

(17) Petz, W.; Kutschera, C.; Heitbaum, M.; Frenking, G.; Tonner, R.; Neumueller, B. *Inorg. Chem.* **2005**, *44*, 1263.

(18) Connor, J. A.; Jones, E. M.; McEwen, G. K.; Lloyd, M. K.; McCleverty, J. A. *J. Chem. Soc., Dalton Trans.* **1972**, 1246.

(19) Angelici, R. J.; Quick, M. H.; Kraus, G. A.; Plummer. D. T. *Inorg. Chem.* **1982**, *21*, 2178.

(20) Cooley, N. A.; MacConnachie, P. T. F.; Baird, M. C. *Polyhedron* **1988**, *7*, 1965.

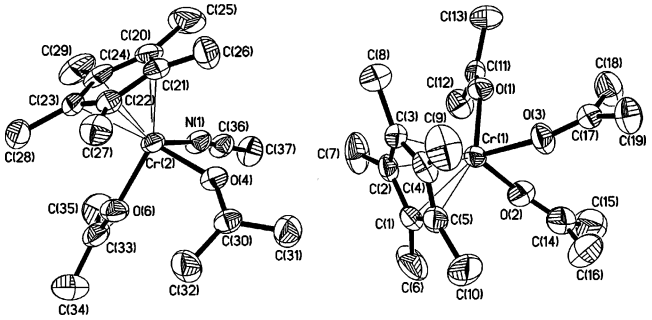

Figure 4. ORTEP diagram for the dications of **7** (50% probability thermal ellipsoids, hydrogen atoms omitted for clarity). Selected bond lengths (Å) and angles (deg): Cr(1)−O(1), 2.005(3); Cr(1)−O(2), 2.012(4); Cr(1)−O(3), 2.020(3); O(1)−Cr(1)−O(2), 91.98(15); O(1)−Cr(1)−O(3), 92.89(14); O(2)−Cr(1)−O(3), 90.78(16); Cr(2)−O(4), 2.010(3); Cr(2)−O(6), 2.000(4); Cr(2)−N(1), 2.044(5); O(4)−Cr(2)−O(6), 95.86(14); O(4)−Cr(2)−N(1), 90.32(15); O(6)−Cr(2)−N(1), 95.74(17).

Scheme 8

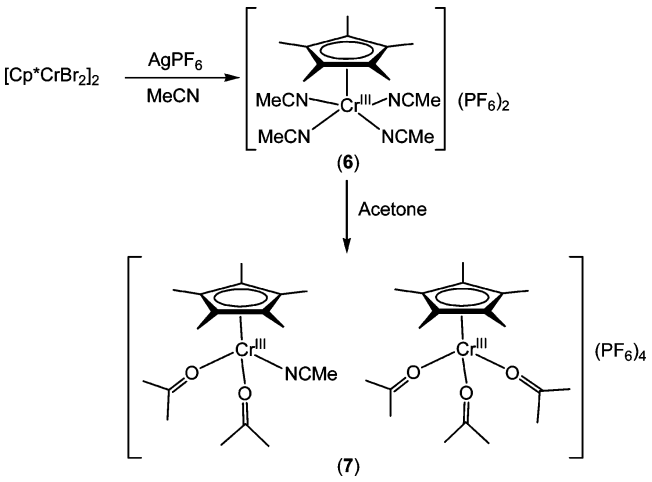

is highly air-sensitive and thermally unstable; hence, elemental analyses were unattainable. Coordination of Cr(III) to four molecules of MeCN was proposed, instead of the normal three, following Köhler's postulation for such a species based on studies of $[CpCr(CNMe)_4]^{2+}$.[21] Since Cr is oxophilic, O-donor solvento ligands may improve the stability of the complex, to give samples amenable to microanalysis and perhaps also yield diffraction-quality crystals. It was found that dissolution and crystallization of **6** in acetone gave dark purple crystals, for which both the microanalytical and X-ray diffraction analysis data indicated a compound consisting of a pair of dicationic Cr complexes, $[Cp^*Cr\{(CH_3)_2CO\}_3][Cp^*Cr\{(CH_3)CO\}_2(MeCN)](PF_6)_4$ (**7**) (see Scheme 8 and the ORTEP diagram in Figure 4).

An instantaneous reaction occurred between **1** and $[Cp^*Cr(CH_3CN)_4](PF_6)_2$ (**6**), generating the complex $[\{(HMB)Ru(\mu\text{-}\eta^2{:}\eta^3\text{-tpdt})\}\{CpCr(NCCH_3)\}](PF_6)_2$ (**8**) in high yield (Scheme 9). An X-ray diffraction analysis confirms that it is isostructural with **5** (Figure 5).

The bond parameters of the Ru−Cr complexes **3**−**5** and **8** are given in Table 1. The Ru−S(thiolato) distances are found in the range 2.369(2)−2.4072(12) Å, compared to 2.3851(10) and 2.3807(10) Å in the precursor complex **1**, while the Ru−S(thioether) distances fall in the range 2.293(2)−2.3166(7) Å, compared to the corresponding bond length of 2.3396(10) Å in

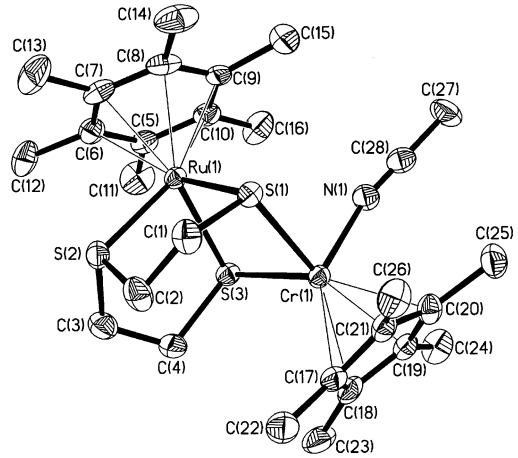

Figure 5. ORTEP diagram for the dication of **8** (50% probability thermal ellipsoids, hydrogen atoms omitted for clarity).

Scheme 9

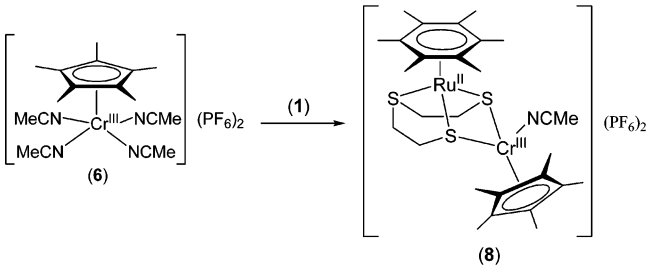

1. The bite angles of the thiolato S atoms at Ru (80.65(2)−86.07(4)°) are much reduced from that (92.18(4)°) in **1**. The Cr−S(thiolato) distances (2.3890(13)−2.4867(8) Å) are comparable to similar bonds (2.295(4)−2.471(3) Å) in the literature,[22] and the S(1)−Cr−S(3) angles (76.57(2)−85.68(5)°) are much larger than the corresponding bite angles (70.333(14)−70.693(19)°) in $CpCr(CO)_2$ complexes containing dithiolato ligands such as bidentate dithiocarbamate.[23]

With the exception of the Ru(II)−Cr(II) complex **4**, the other Ru(II)−Cr complexes (**3**, **5**, and **8**) containing Cr in the 0 or +3 oxidation state are air-stable as solids or in solution in acetonitrile for several days (complex **3**) and for an extended period (**5** and **8**).

Electrochemistry Studies. The cyclic voltammetric responses observed for CH_3CN solutions containing 0.5 mM **3**, **4**, **5**, and **8** varied considerably depending on the electrode surface and temperature. Figure 6 displays voltammograms recorded at a GC electrode, where the electrochemical responses were generally the finest. The rates of heterogeneous electron transfer were often very slow on Pt electrodes, resulting in a large potential difference between the anodic (E_p^{ox}) and cathodic (E_p^{red}) peaks and very broad peak shapes.

3 displayed three oxidation processes on a GC electrode at 243 K (Figure 6a). At 293 K the second more positive process at −0.06 V had an anodic to cathodic peak current ratio (i_p^{ox}/i_p^{red}) ≫ 1, indicating chemical instability of the double oxidized compound at higher temperatures. On the Pt electrode at 243 K, the first process appeared the same as on the GC electrode, but the second process had a much wider peak-to-peak separation, suggesting slow heterogeneous electron transfer or a strong interaction with the electrode surface. Interestingly, at 293 K

(21) Heigl, O. M.; Herdtweck, E.; Grasser, S.; Köhler, F. H.; Strauss, W.; Zeh, H. *Organometallics* **2002**, *21*, 3572 and ref 7b therein.

(22) Goh, L. Y.; Tay, M. S.; Mak, T. C. W.; Wang, R.-J. *Organometallics* **1992**, *11*, 1711 and references therein.

(23) Goh, L. Y.; Weng, Z.; Leong, W. K.; Leung, P. H. *Organometallics* **2002**, *21*, 4398.

Table 1. Selected Bond Lengths (Å) and Angles (deg) of Ru−Cr Complexes

3		**4**		**5**		**8**	
Ru(1)−S(1)	2.369(2)	Ru(1)−S(1)	2.3722(7)	Ru(1)−S(1)	2.3838(12)	Ru(1)−S(1)	2.3772(11)
Ru(1)−S(2)	2.293(2)	Ru(1)−S(2)	2.3166(7)	Ru(1)−S(2)	2.3032(12)	Ru(1)−S(2)	2.3063(13)
Ru(1)−S(3)	2.374(2)	Ru(1)−S(3)	2.3700(7)	Ru(1)−S(3)	2.3870(12)	Ru(1)−S(3)	2.4072(12)
Cr(1)−S(1)	2.477(3)	Cr(1)−S(1)	2.4867(8)	Cr(1)−S(1)	2.3890(13)	Cr(1)−S(1)	2.3937(14)
Cr(1)−S(3)	2.475(2)	Cr(1)−S(3)	2.4663(7)	Cr(1)−S(3)	2.3927(14)	Cr(1)−S(3)	2.4077(13)
Cr(1)−C(17)	1.886(9)	Cr(1)−C(22)	1.845(3)	Cr(1)−Cl(1)	2.2745(14)	Cr(1)−N(1)	2.071(4)
Cr(1)−C(18)	1.870(10)	Cr(1)−C(23)	1.848(3)				
Cr(1)−C(19)	1.798(10)	Cr(2)−C(29)	1.815(3)				
Cr(1)−C(20)	1.895(8)	Cr(2)−C(30)	1.820(3)				
		Cr(2)−C(31)	1.817(3)				
S(1)−Ru(1)−S(2)	86.41(8)	S(1)−Ru(1)−S(2)	87.24(3)	S(1)−Ru(1)−(2)	85.95(4)	S(1)−Ru(1)−S(2)	86.91(5)
S(1)−Ru(1)−S(3)	83.41(7)	S(1)−Ru(1)−S(3)	80.65(2)	S(1)−Ru(1)−(3)	86.07(4)	S(1)−Ru(1)−S(3)	86.05(4)
S(2)−Ru(1)−S(3)	86.48(8)	S(2)−Ru(1)−S(3)	85.17(2)	S(2)−Ru(1)−(3)	85.96(4)	S(2)−Ru(1)−S(3)	85.57(5)
S(1)−Cr(1)−S(3)	79.17(7)	S(1)−Cr(1)−S(3)	76.57(2)	S(1)−Cr(1)−S(3)	85.82(5)	S(1)−Cr(1)−S(3)	85.68(5)
S(1)−Cr(1)−C(18)	93.7(3)	S(1)−Cr(1)−C(22)	80.58(9)	S(1)−Cr(1)−Cl(1)	88.57(5)	S(1)−Cr(1)−N(1)	90.76(13)
S(3)−Cr(1)−C(19)	95.4(3)	S(3)−Cr(1)−C(23)	80.79(9)	S(3)−Cr(1)−Cl(1)	93.09(5)	S(3)−Cr(1)−N(1)	91.82(12)
C(18)−Cr(1)−C(19)	91.5(4)	C(22)−Cr(1)−C(23)	79.63(14)				
C(17)−Cr(1)−C(20)	167.6(4)	C(29)−Cr(2)−C(30)	87.95(14)				
		C(29)−Cr(2)−C(31)	92.10(15)				
		C(30)−Cr(2)−C(31)	89.69(13)				

the second process could barely be detected on Pt and instead appeared as a long gradual sloping current response that extended to the third process at +1.09 V. It is difficult to determine the molecular position of the oxidation, since both Ru(II) and Cr(0) are expected to be readily oxidized. A reduction process was detected on Pt and GC electrodes for solutions of **3** at negative potentials (at high and low temperatures), with a current magnitude similar to that of the oxidation processes, suggesting that the same number of electrons were transferred. Considering that, in **3**, Cr exists in an oxidation state of 0, it is more likely that the reduction process is associated with transformation of Ru(II) to Ru(I).

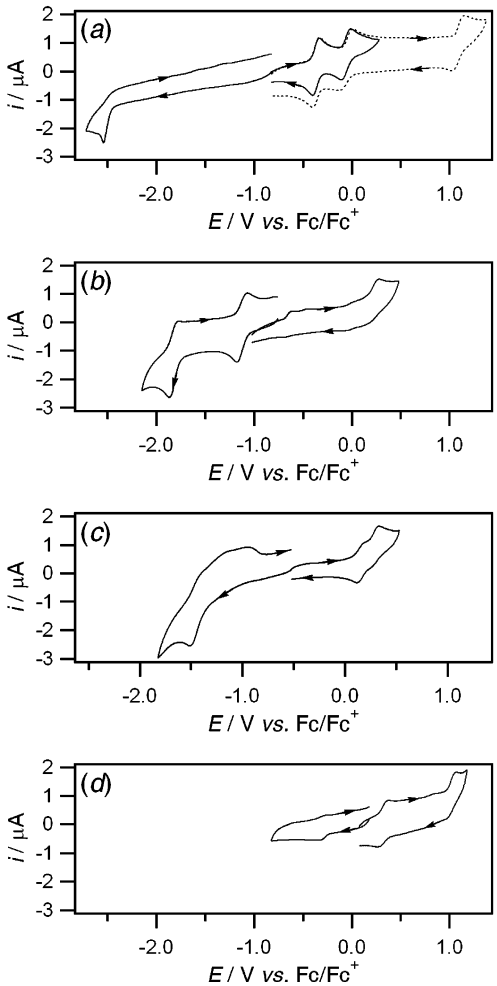

Figure 6. Cyclic voltammograms of 0.5 mM substrates recorded at a 1 mm GC electrode in CH_3CN with 0.25 M Bu_4NPF_6 at a scan rate of 100 mV s^{-1}: (a) **3** at $T = 243$ K, (b) **4** at $T = 293$ K, (c) **5** at $T = 243$ K, and (d) **8** at $T = 243$ K. The dashed line in (a) is the voltammogram obtained when the scan is extended to more positive potentials.

Cyclic voltammograms at a GC electrode of solutions containing **4** showed two oxidation processes at negative potentials at 293 K (Figure 6b). At 243 K the first oxidation process displayed a very wide peak-to-peak (ΔE_{pp}) separation, but the second more positive process had a ΔE_{pp} value very similar to that observed at 293 K. On Pt electrodes, both oxidation processes had very broad peaks with large ΔE_{pp} values (several hundred millivolts), suggesting slow rates of heterogeneous electron transfer or complicated solute−electrode interactions. A complicated chemically irreversible oxidation process was evident on both electrodes at approximately +0.37 V, which could be due to either the heterobimetallic cation or the Cr^0 anion.

5 displayed two closely spaced, one-electron chemically reversible oxidation processes at positive potentials (Figure 6c and Table 2). One chemically irreversible reduction process was evident at −1.52 V, with the current response approximately 2 times greater than the current obtained for the individual oxidation responses, therefore representing a multiple-electron reduction. The voltammograms were similar on Pt and GC electrodes at high and low temperatures. An adsorption peak was evident on both electrodes (particularly pronounced on the GC electrode) before and after the main diffusion-controlled electrochemical reduction response.

On a GC electrode at 243 K, **8** displayed one chemically reversible oxidation process at +0.32 V and another chemically irreversible process of a similar current magnitude at +1.08 V (Figure 6d). A partially chemically reversible process was evident at −0.30 V. At 293 K all processes appeared chemically irreversible. On Pt electrodes the processes appeared to suffer from very slow heterogeneous electron transfer at high and low temperatures, as only widely spaced and broad-shaped peaks were detected during oxidative and reductive scans.

Compounds **5** and **8** contain metal ions in the same oxidation state and geometry (although the complexes have a different overall charge) and, therefore, would be expected to have similar

Table 2. Cyclic Voltammetric Data Obtained at a Scan Rate of 0.1 V s^{-1} at 1 mm Diameter GC or Pt Electrodes at 243 or 293 K in CH_3CN with 0.25 M Bu_4NPF_6 as the Supporting Electrolyte

	reduction processes[e]				oxidation processes[e]			
compd	E_p^{red} [f]/V	E_p^{ox} [g]/V	$E^r_{1/2}$ [h]/V	ΔE^i/mV	E_p^{ox} [g]/V	E_p^{red} [f]/V	$E^r_{1/2}$ [h]/V	ΔE^i/mV
3[a,c]					−0.328	−0.398	−0.36	73
					−0.007	−0.106	−0.06	99
					+1.157	+1.025	1.09	132
4[a,d]	−1.270	−1.153	−1.21	117				
	−2.018	−1.914	−1.97	104				
					−0.37			
5[b,d]	−1.52							
					+0.20	+0.105	+0.15	95
					+0.348	+0.27	+0.31	78
8[a,c]	−0.340	−0.25	−0.30	90				
					+0.380	+0.258	+0.32	122
					+1.08			

[a] GC electrode. [b] Pt electrode. [c] Temperature 243 K. [d] Temperature 293 K. [e] All potentials are relative to the Fc/Fc^+ redox couple. [f] E_p^{red} = reductive peak potential. [g] E_p^{ox} = oxidative peak potential. [h] $E^r_{1/2} = (E_p^{red} + E_p^{ox})/2$. [i] $\Delta E = |E_p^{ox} - E_p^{red}|$.

electrochemical characteristics. Both compounds show two one-electron oxidation processes, although for **8** the second oxidation process is chemically irreversible at a scan rate of 100 mV s^{-1} and occurs at a considerably higher potential than the first process (compare parts c and d of Figure 6).

3. Conclusion

The first examples of dithiolato-bridged Ru−Cr bimetallic complexes, containing Cr in the 0, +2, and +3 oxidation states, have been synthesized from the reaction of $(HMB)Ru^{II}(\eta^3\text{-tpdt})$ with chromium complexes in various oxidation states. The compounds could be electrochemically oxidized and reduced in several heterogeneous electron-transfer steps. For most compounds the cyclic voltammetric responses were complicated and varied depending on the electrode surface and temperature. Compound **3** could be oxidized in three chemically reversible one-electron processes, most likely involving both the Ru and Cr ions.

4. Experimental Section

4.1. General Procedures. These were as described in an earlier paper.[11] The compounds $[(HMB)Ru^{II}(\eta^3\text{-tpdt})]$ (**1**),[8] $[CpCrCl_2(SPyH)]$,[24] $[Cp^*CrBr_2]_2$,[25] and $[CpCr(CO)_3]_2$ ($Cp = \eta^5\text{-}C_5H_5$)[26] were prepared as previously reported. CH_3CN was distilled from calcium hydride and MeOH from freshly generated magnesium methoxide before use. All other solvents were distilled from sodium benzophenone ketyl.

4.2. Reaction of 1 with $Cr(CO)_6$. To a stirred solution of **1** (20 mg, 0.048 mmol) in methanol (8 mL) was added $Cr(CO)_6$ (12 mg, 0.055 mmol). No reaction was observed even after 2 h. The reaction mixture was cooled in an ice bath and then irradiated with UV light (λ = 350 nm) for 1.5 h, whereupon precipitation of orange solids of $[\{(HMB)Ru(\mu\text{-}\eta^2\text{:}\eta^3\text{-tpdt})\}\{Cr(CO)_4\}]$ (**3**) occurred. After irradiation for an additional 1.5 h, the solids were filtered and recrystallized from THF/hexane. Air-stable orange crystals (8 mg, 29%) of **3** were obtained after 24 h at −30 °C.

Data for 3. ^1H NMR (δ, CD_3CN): SCH_2, 3.53−3.45 (seven-line m, 2H), 2.86−2.77 (five-line m, 2H), 2.50−2.42 (five-line m, 2H), 2.15−2.08 (seven-line m, 2H); C_6Me_6, 2.06 (s, 18H). ^{13}C NMR (δ, CD_3CN): *C*O, 227.6; C_6Me_6, 100.3; SCH_2, 41.2, 32.3; C_6Me_6, 15.2. FAB^+ MS: *m*/*z* 580 $[M]^+$, 552 $[M - CO]^+$, 496 $[M - 3CO]^+$, 468 $[M - 4CO]^+$. IR (ν (cm^{-1}), KBr): 2921 m, 2852 w, 1986 s (C≡O), 1851 vs (C≡O), 1817 vs (C≡O), 1444 w, 1421 w, 1407 w, 1386 w, 1160 vw, 1115 vw, 1071 w, 1016 w, 938 vw, 920 vw, 830 w, 809 vw, 689 m, 649 m, 633 m, 479 m. Anal. Found: C, 41.3; H, 4.4; S, 17.0. $C_{20}H_{26}CrO_4RuS_3$ requires C, 41.4; H, 4.5; S, 16.6.

4.3. Reaction of 1 with $[CpCr(CO)_3]_2$. To a stirred red solution of **1** (51 mg, 0.13 mmol) in toluene (10 mL) was added solid $[CpCr(CO)_3]_2$ (46 mg, 0.11 mmol). Brown solids of $[\{(HMB)Ru(\mu\text{-}\eta^2\text{:}\eta^3\text{-tpdt})\}\{CpCr(CO)_2\}][CpCr(CO)_3]$ (**4**) started to precipitate after ca. 3 h. After an additional 3 h, the solids were filtered and washed with toluene (3 mL) (31 mg, 35% yield). Stirring the mother liquor for another 18 h gave a second crop of the shiny brown particles upon filtration (28 mg, 32% yield). Diffusion of ether into an acetonitrile solution of **4** gave diffraction-quality crystals after 1 week at −30 °C.

Data for 4. ^1H NMR (δ, CD_3CN): C_5H_5, 5.09, 4.41 (each s, 5H); SCH_2, 3.52−3.45 (eight-line m, 2H), 3.08−2.98 (six-line m, 2H), 2.58−2.50 (eight-line m, 2H), 1.88−1.78 (eight-line m, 2H); C_6Me_6, 2.13 (s, 18H). ^{13}C NMR (δ, CD_3CN): *C*O, 266.2, 246.8; C_6Me_6, 101.9; C_5H_5, 96.0, 82.6; SCH_2, 44.3, 34.8; C_6Me_6, 15.6. FAB^+ MS: *m*/*z* 589 $[M]^+$, 533 $[M - 2CO]^+$, 477 $[M - 2CO - 4CH_2]^+$, 416 $[M - CpCr(CO)_2]^+$. IR (ν (cm^{-1}), KBr): 3102 w, 2924 w, 1944 vs (C≡O), 1882 vs (C≡O), 1867 ssh (C≡O), 1757 vs (C≡O), 1420 w, 1387 w, 1161 vw, 1126 vw, 1111 vw, 1067 w, 1009 w, 939 vw, 867 vw, 827 w, 793 w, 692 w, 652 m, 633 w, 573 w, 543 w, 508 w, 471 w. Anal. Found: C, 46.6; H, 4.6; S, 12.0. $C_{31}H_{36}Cr_2O_5RuS_3$ requires C, 47.1; H, 4.6; S, 12.2.

4.4. Reaction of 1 with $[CpCrCl_2(SPyH)]$. Into a solid mixture of **1** (15 mg, 0.036 mmol) and $[CpCrCl_2(SPyH)]$ (11 mg, 0.037 mmol) was injected acetonitrile (10 mL). The solution was stirred for 2 h, and the precipitated green solids were filtered using a Por. 4 glass sinter. The solids were dissolved in MeCN (8 mL), and PF_6 metathesis was carried out by stirring with NH_4PF_6 (15 mg, 0.092 mmol) for 15 min. After filtration of the suspension, the filtrate was concentrated to half-volume, and ether was added. Air-stable green solids of $[\{(HMB)Ru(\mu\text{-}\eta^2\text{:}\eta^3\text{-tpdt})\}\{CpCrCl\}](PF_6)$ (**5**) (16 mg, 62%) were obtained after 2 days at −30 °C.

Data for 5. ^1H NMR (δ, CD_3CN): 8.02 (br s, $\nu_{1/2}$ = ca. 120 Hz), 7.34 (br s, $\nu_{1/2}$ = ca. 90 Hz). FAB^+ MS: *m*/*z* 568 $[M - PF_6]^+$. FAB^- MS: *m*/*z* 145. IR (ν (cm^{-1}), KBr): 2958 wsh, 2921 m, 2854 w, 1431 m, 1410 m, 1388 m, 1261 w, 1130 w, 1072 w, 1015 m, 841 vs (PF_6), 558 v (PF_6). Anal. Found: C, 35.4; H, 4.9; S, 13.6. $C_{21}H_{31}ClCrF_6PRuS_3$ requires C, 35.4; H, 4.4; S, 13.5.

4.5. Synthesis of $[Cp^*Cr(CH_3CN)_4](PF_6)_2$ (6). To a solid mixture of $[Cp^*CrBr_2]_2$ (32 mg, 0.046 mmol) and $AgPF_6$ (49 mg, 0.19 mmol) was added acetonitrile (8 mL). An instantaneous reaction took place, resulting in a drastic color change from dark blue to red, with the concurrent precipitation of white solids of

(24) Ng, W. L. V.; Leong, W. K.; Koh, L. L.; Tan, G. K.; Goh, L.Y. *J. Organomet. Chem.* **2004**, *689*, 3210.
(25) Morse, D. B.; Rauchfuss, T. B.; Wilson, S. R. *J. Am. Chem. Soc.* **1988**, *110*, 8234.
(26) Manning, A. R.; Hackett, P.; Birdwhistell, R.; Soye, P. *Inorg. Synth.* **1990**, *28*, 148.

Table 3. Data Collection and Processing Parameters

complexes	**3**	**4**	**5**	**7**	**8**
empirical formula	$C_{24}H_{34}CrO_5RuS_3$	$C_{31}H_{36}Cr_2O_5RuS_3$	$C_{25}H_{39}ClCrF_6OPRuS_3$	$C_{37}H_{63}Cr_2F_{24}NO_5P_4$	$C_{28}H_{44}CrF_{12}NP_2RuS_3$
mol wt	651.76	789.85	785.23	1285.76	933.83
temp (K)	223(2)	293(2)	223(2)	223(2)	223(2)
cryst size (mm^3)	0.38 × 0.32 × 0.26	0.50 × 0.46 × 0.30	0.24 × 0.14 × 0.04	0.28 × 0.20 × 0.10	0.28 × 0.20 × 0.18
cryst syst	monoclinic	triclinic	monoclinic	triclinic	orthorhombic
space group	*P*2(1)/*c*	$P\bar{1}$	*P*2(1)/*c*	$P\bar{1}$	*P*2(1)2(1)2(1)
a (Å)	9.5514(6)	11.5868(2)	8.8705(5)	10.5066(5)	12.5994(6)
b (Å)	12.4532(7)	14.5284(3)	25.8348(15)	16.2114(8)	13.0396(7)
c (Å)	22.7720(14)	18.7799(3)	13.5751(8)	18.1051(9)	21.6305(11)
α (deg)	90	88.7210(10)	90	110.2040(10)	90
β (deg)	91.5950(10)	86.6820(10)	105.5260(10)	105.0970(10)	90
γ (deg)	90	81.9140(10)	90	91.6270(10)	90
cell vol ($Å^3$)	2707.6(3)	3124.37(10)	2997.4(3)	2770.2(2)	3553.7(3)
Z	4	4	4	2	4
D_{calcd} (g cm^{-3})	1.599	1.679	1.740	1.541	1.745
abs coeff (mm^{-1})	1.223	1.400	1.275	0.627	1.083
F(000) electrons	1336	1608	1596	1312	1892
θ range for data collection (deg)	1.86−25.00	1.77−26.37	1.58−27.49	1.25−25.00	1.82−27.50
index ranges	$-11 \le h \le +11$	$-14 \le h \le +9$	$-10 \le h \le +11$	$-12 \le h \le +12$	$-13 \le h \le +16$
	$-13 \le k \le +14$	$-17 \le k \le +18$	$-33 \le k \le +29$	$-19 \le k \le +19$	$-16 \le k \le +14$
	$-23 \le l \le +27$	$-23 \le l \le +23$	$-17 \le l \le +14$	$-21 \le l \le +21$	$-28 \le l \le +22$
no. of reflns collected	15222	17530	21185	30047	25215
no. of independent reflns	4761	12062	6888	9767	8172
max and min transm	0.7417 and 0.6537	0.6791 and 0.5159	0.9508 and 0.7494	0.9400 and 0.8440	0.8289 and 0.7513
no. of data/restraints/params	4761/81/299	12062/0/758	6888/6/349	9767/104/ 805	8172/0/445
final *R* indices [$I > 2\sigma(I)$][a,b]	R1 = 0.0803	R1 = 0.0306	R1 = 0.0514	R1 = 0.0755	R1 = 0.0493
	wR2 = 0.1595	wR2 = 0.0743	wR2 = 0.1007	wR2 = 0.1938	wR2 = 0.1070
R indices (all data)	R1 = 0.0992	R1 = 0.0408	R1 = 0.0960	R1 = 0.1106	R1 = 0.0580
	wR2 = 0.1668	wR2 = 0.0792	wR2 = 0.1130	wR2 = 0.2179	wR2 = 0.1107
GOF[c]	1.306	1.020	0.961	1.031	1.052
largest diff peak and hole (e $Å^{-3}$)	0.910 and −1.131	0.575 and −0.510	0.798 and −0.652	0.888 and −0.438	1.875 and −0.534

[a] $R1 = (\sum|F_o| - |F_c|)\sum|F_o|$. [b] $wR2 = [(\sum\omega|F_o| - |F_c|)^2/\sum\omega|F_o|^2]^{1/2}$. [c] $GOF = [(\sum\omega|F_o| - |F_c|)^2/(N_{obsd} - N_{param})]^{1/2}$.

AgBr. After being stirred for 1.5 h, the solution was filtered over a glass sinter (Por. 4) to remove the precipitated AgBr and the excess $AgPF_6$. The red filtrate was concentrated and ether added. Red powdery solids of **6** (38 mg, 64%) were obtained after 2 days at −30 °C.

Complex **6** is very air-sensitive and slowly decomposes at room temperature under argon to an uncharacterizable blue solid. In acetone, an immediate color change from red to deep blue was observed. Diffusion of ether into the solution at −30 °C for 1 week gave dark purple crystals of complex $[Cp^*Cr\{(CH_3)_2CO\}_3][Cp^*Cr\{(CH_3)CO\}_2(MeCN)](PF_6)_4$ (**7**).

Data for 6. ^1H NMR (*δ*, CD_3CN): C_5H_5, 5.23 (vbr s, $\nu_{1/2}$ = ca. 210 Hz); *Me*CN, −37.71 (vbr s, $\nu_{1/2}$ = ca. 870 Hz). IR (ν (cm^{-1}), KBr): 2976 br m, 2915 s, 2303 m (C≡N), 2274 s (C≡N), 1481 m, 1425 m, 1377 m, 1360 m, 1260 w, 1154 w, 1071 w, 1023 m, 834 br vs (PF_6), 561 vs (PF_6), 429 m. Microanalytical data are not available, owing to the extreme air and thermal instability.

Data for 7. IR (ν (cm^{-1}), KBr): 2965 vw, 2914 w, 2857 vw, 2292 vw (C≡N), 2280 w (C≡N), 1708 w (C≡O), 1670 m (C≡O), 1483 m, 1426 m, 1375 m, 1251 w, 1157 vw, 1093 vw, 1080 vw, 1023 m, 835 vs (PF_6), 560 s (PF_6), 432 m. FAB^+ MS: *m*/*z* mother ion not observed. FAB^- MS: *m*/*z* 145. Anal. Found: C, 28.5; H, 4.0; N, 1.5. $C_{27}H_{43}NCr_2F_{24}O_5P_4$ requires C, 28.3; H, 3.8; N, 1.2.

4.6. Reaction of 1 with 6. Into a solid mixture of **1** (18 mg, 0.043 mmol) and **6** (28 mg, 0.044 mmol) was injected acetonitrile (10 mL). An instantaneous reaction took place, giving a dark brown solution which was stirred for an hour. The solution was filtered to remove any solid residue, but none was obtained from the filtration. The filtrate was concentrated to half-volume (5 mL), and ether was added; the solution was then cooled at −30 °C. Black crystalline solids of $[\{(HMB)Ru(\mu\text{-}\eta^2\text{:}\eta^3\text{-tpdt})\}\{Cp^*Cr(MeCN)\}](PF_6)_2$ (**8**) (32 mg, 79%) were obtained after 12 h.

Data for 8. ^1H NMR (*δ*, CD_3CN): 7.76 (br s, $\nu_{1/2}$ = ca. 150 Hz), 6.83 (br s, $\nu_{1/2}$ = ca. 105 Hz). ESI^+ MS: *m*/*z* mother ion not observed, 825, 799, 706, 690, 663, 635 [fragments not assignable], 416 $[(C_6Me_6)Ru(C_4H_8S_3)]^+$, 187 $[Cp^*Cr]^+$. ESI^- MS: *m*/*z* 145. IR (ν (cm^{-1}), KBr), 2998 wsh, 2936 w, 2312 w (C≡N), 2274 m (C≡N), 1947 w, 1885 w, 1758 w, 1489 m, 1428 m, 1382 m, 1288 vw, 1164 vw, 1072 m, 1020 m, 838 vs (PF_6), 743 vw, 558 s (PF_6), 436 w. Anal. Found: C, 36.3; H, 4.9; N, 1.5; S, 10.3. $C_{28}H_{44}CrF_{12}NP_2RuS_3$ requires C, 36.0; H, 4.8; N, 1.5; S, 10.3.

4.7. X-ray Crystal Structure Determinations. The crystals were mounted onto glass fibers. X-ray data were collected on a Bruker AXS SMART APEX CCD diffractometer, using Mo Kα radiation (λ = 0.71073 Å), at 223 or 293 K. The program SMART[27] was used for collecting the intensity data, indexing, and determination of lattice parameters, SAINT[28] was used for integration of the intensity of reflections and scaling, SADABS[29] was used for absorption correction, and SHELXTL[30] was used for space group and structure determination and least-squares refinements against F^2.

The structures were solved by direct methods to locate the heavy atoms, followed by difference maps for the light, non-hydrogen atoms. The hydrogens were placed in calculated positions. The asymmetric unit of the crystal of **3** contains one molecule of **3**, which shows disorder in the methylene carbons (C2 and C4) of the tpdt ligand, splitting into two sets of positions with a 50:50 occupancy ratio. Complex **5** shows a similar disorder in the methylene carbons C1 and C3, which are split into two sets of positions with occupancy ratio 55:45. There is also one THF molecule present as a space-filling solvent in complexes **3** and **5**. The asymmetric unit of the crystal of **7** contains two cations and four anions. Fluorine atoms of three of the PF_6^- anions are disordered. The crystal data collection and processing parameters for **3**−**5**, **7**, and **8** are given in Table 3.

Acknowledgment. Support from the National University of Singapore via Academic Research Fund Grant No. R143-000-135/209-112 (L.Y.G.) and research scholarships to R.Y.C.S. and V.W.L.N. is gratefully acknowledged.

Supporting Information Available: Crystallographic data as CIF files of **3**−**5**, **7**, and **8**. This information is available free of charge via the Internet at http://pubs.acs.org.

OM700474K

(27) *SMART*, version 5.628; Bruker AXS Inc.: Madison, WI, 2001.
(28) *SAINT*, version 6.22a; Bruker AXS Inc.: Madison, WI, 2001.
(29) Sheldrick, G. M. SADABS, 1996.
(30) *SHELXTL*, version 5.1; Bruker AXS Inc.: Madison, WI, 1997.